Cellulose–Chitosan Interpenetrating Polymer Network for Electro-Active Paper Actuator

Zhijiang Cai, Jaehwan Kim

Center for EAPap Actuator, Department of Mechanical Engineering, Inha University, Nam-Ku, Incheon 402-751, South Korea

Received 31 March 2008; accepted 22 March 2009
DOI 10.1002/app.30456
Published online 2 June 2009 in Wiley InterScience (www.interscience.wiley.com).

ABSTRACT: In this article, the cellulose-chitosan interpenetrating polymer network (IPN) films were prepared and fabricated as the electro-active paper actuator. The characteristics of the cellulose–chitosan IPN films were examined by SEM, FT-IR, XRD, DSC, and tensile test. The performance of the IPNs based actuator was evaluated in terms of bending displacement with respect to the actuation frequency, voltages, humidity levels, chitosan content, and time variation. It was observed that with chitosan content increasing in the IPNs, the crystallinity decreased and the network became denser, which caused the Young's modulus to increase. Chitosan content in IPNs also significantly affected the bending performance. The optimum IPN weight ratio of cellulose and chitosan was 60 : 40. The maximum bending displacement of 7.2 mm was found at 80% relative humidity level. In terms of durability, the bending lifetime at 70% humidity level was about 10 h with 17% performance degradation. More issues on the actuator performance and durability are addressed. © 2009 Wiley Periodicals, Inc. J Appl Polym Sci 114: 288–297, 2009

Key words: electro-active paper; cellulose; chitosan; interpenetrating polymer network; bending performance; durability

INTRODUCTION

Cellulose, as an environmentally friendly and renewable biomaterial, constitutes about 2×10^{12} tons of the total annual biomass production photosynthesized by carbon dioxide fixation on land and in sea.[1] Cellulose has a basic molecular unit of $C_6H_{10}O_5$ linked in the form of β-1,4-glucan. Each chain unit of cellulose contains three hydroxyl groups, which make cellulose a hydrophilic material. Cellulose is mostly obtained from wood pulps, cottons, and sea plants. Numerous applications of cellulose take advantage of its biocompatibility and chirality for the immobilization of proteins and antibodies, the separation of enantiomeric molecules, as well as the formation of cellulose composites with synthetic polymers and biopolymers.

The discovery of an electromechanical coupling effect in wood dates back to 1950, when Bazhenov reported a piezoelectric response in wood.[2] Fukada experimentally verified the piezoelectric coefficients of wood, and demonstrated that oriented cellulose crystallites were responsible for the observed shear piezoelectricity.[3] These research results imply that cellulose has the potential to be used in sensor or actuator field. Recently, cellulose paper has been discovered as a smart material actuating with electric field.[4] Cellulose paper was prepared form cellulose fibers. These fibers were dissolved into a solvent and cast as a sheet. Thin gold electrodes were deposited on both sides of the cellulose paper, and when an electric field was applied across the thickness of the paper, it showed a bending deformation. This cellulose paper was termed as The Electro-Active Paper (EAPap).[5] Cellulose EAPap has merits as a smart material in terms of lightweight, dryness, biodegradability, abundance, low price, large displacement output, and low actuation voltage. Possible application areas of this material are micro-insect robots, flying objects, flying magic paper, flower-robots, smart wallpaper, e-papers, and micro-electromechanical system sensors. However, this material is very sensitive to humidity, its maximum bending performance was shown at high humidity condition, and its performance is degraded with time.[6]

To improve the performance of EAPap actuator, polypyrrol and polyaniline conductive polymers were coated on the cellulose EAPap.[7,8] The conductive polymer-coated EAPap actuator exhibited a large displacement output, but it was still sensitive to humidity, and the degradation was not improved. Another attempt was to mix carbon nanotubes (CNT) with cellulose to improve the performance of EAPap as a bending actuator.[9–11] This CNT-mixed

Correspondence to: J. Kim (jaehwan@inha.ac.kr).
Contract grant sponsor: Creative Research Initiatives (EAPap Actuator) of KOSEF/MEST.

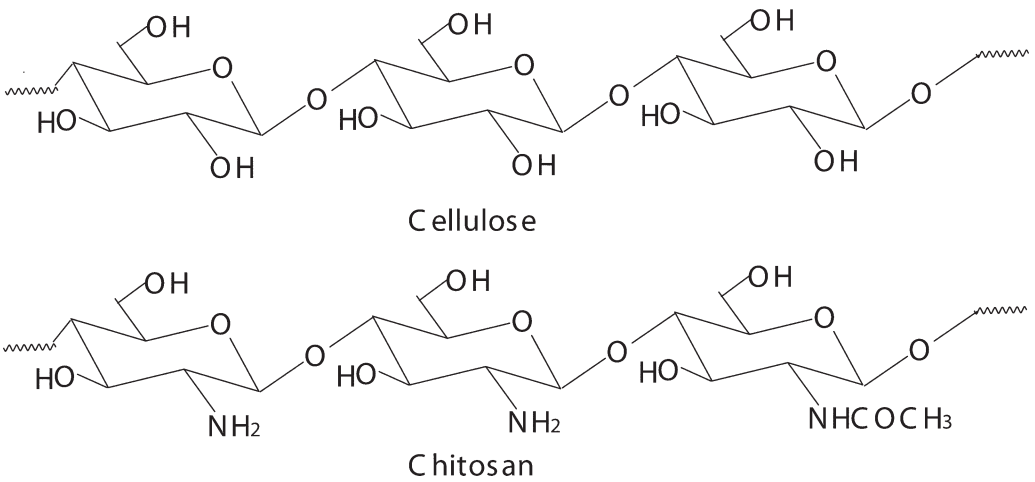

Figure 1 The molecular structure of cellulose and chitosan.

cellulose EAPap increased the mechanical power output and the resonance frequency, but it was also still sensitive to humidity.

Chitosan, a copolymer of glucosamine and *N*-acetylglucosamine unit linked by 1,4-glucosidic bonds, is obtained by N-deacetylation of chitin. Chitosan is a biocompatible polymer, reported to exhibit a great variety of useful biological properties. Chitosan has amino groups and hydroxyl groups on its backbone, which on the one hand makes chitosan itself hydrophilic, and on the other hand brings chitosan a polycationic property.[12] The molecular structures of cellulose and chitosan are very similar as seen in Figure 1. In our previous research,[13] we used cellulose–chitosan laminated films as EAPap actuators. The results showed maximum bending displacement at 60% relative humidity (RH), which is promising to reduce the humidity sensitivity.

In this article, an EAPap actuator based on cellulose–chitosan interpenetrating polymer network (IPN) is prepared to improve the actuator performance of EAPap in terms of bending displacement, durability, and humidity effect. Details of the cellulose–chitosan IPN EAPap actuator fabrication are delineated. The characteristics of cellulose–chitosan IPNs are evaluated by FT-IR, X-ray diffraction (XRD), differential scanning calorimety (DSC), and tensile test. The actuator performance of the EAPap actuator is tested in terms of free bending displacement with respect to the actuation frequency, voltage, humidity levels, and time variations.

EXPERIMENTAL

Materials

Cotton cellulose (MVE, DPw = 7450) was purchased from Buckeye Technologies Co. (USA). Chitosan (medium molecular weight, Brookfield viscosity 200–800 cP, 75–85% deacetylated) was purchased from Aldrich (St. Louis, MO). Hydrochloric acid (36.5–38 wt %) was purchased from Sigma-Aldrich. Trifluoroacetic acid (>99 wt %) was purchased from Daejung Chemical & Metals Co. Sodium hydroxide (bead, 98 wt %) was purchased from Samchun Pure Chemical Co. Glutaraldehyde (solution Grade II, 25 wt % in H_2O) was purchased from Sigma-Aldrich.

Preparation of cellulose–chitosan IPN films

Cotton cellulose was cut into small pieces, soaked into water overnight, squeezed, and filtered to remove the water. The same process was performed four times with methanol and one time with acetone. The treated cotton cellulose and chitosan powder were heated under reduced pressure at 110°C for 2 h. Then the cotton cellulose was mixed with chitosan powder at different weight ratios and dissolved in trifluoroacetic acid (99 wt %) at room temperature. The transparent cellulose–chitosan blend solution was kept in a sealed glass bottle. The clear blend solution was spincoated on wafer and dried at room temperature for 12 h. To ensure complete elimination of the solvent, the films were then dried at 60°C for 6 h. Transparent films were obtained by peeling them off from the wafer. The films were soaked in an aqueous solution of NaOH (0.4 wt %) at room temperature for 6 h to remove the acids. They were then washed with running tap water and immersed in deionized water for 4 h. Washing the films with running water was assumed to remove all Na^+ ions that remained in the films. The cellulose–chitosan blend films were immersed in glutaraldehyde solution containing 0.3% (wt %) HCl for 6 h for conducting the cross linking reaction. The concentration of the glutaraldehyde solution is 0.02% (wt %). And the total amount of glutaraldehyde is about 10 wt % relative to the cellulose–chitosan blend film. Then, the films were washed with

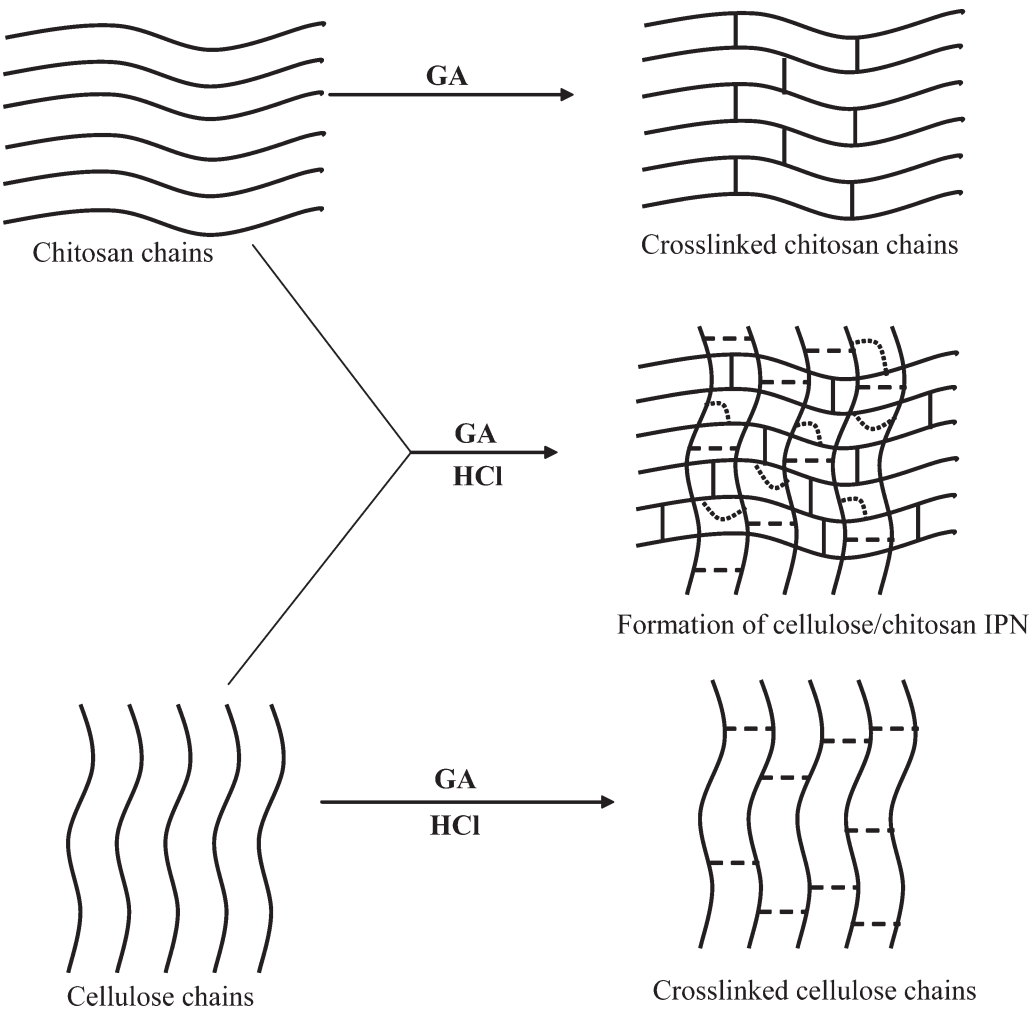

Figure 2 Schematic representation of the synthesis of cellulose–chitosan IPN.

deionized water to remove the unreacted glutaraldehyde. The films were vacumm dried at 40°C for 24 h and stored in a desiccator. A schematic representation of the synthesis of IPN is given in Figure 2.

Gold electrode coating

To prepare the EAPap actuator, gold electrodes were deposited on both sides of the cellulose–chitosan IPN film using a physical vapor deposition system. The size of the EAPap sample was 10 × 40 mm. The thickness of the gold electrodes was much thin (0.1 μm) that the gold electrodes did not significantly affect the bending stiffness of the actuator. The thickness of the sample films is around 10 ± 2 μm.

Characterization

FT-IR spectra were obtained using a Perkin-Elmer System 2000 FT-IR spectrophotometer. The film was cut into pieces and grounded with KBr pellets. XRD pattern were recorded on an X-ray diffractometer (D/MAX-2500, Rigaku), using Cu Kα radiation at 40 kV and 30 mA. The diffraction angle ranged from 5 to 40°. DSC (DSC 200 F3, NETZSCH) test was performed on cellulose–chitosan IPNs. Samples were heated from room temperature to 400°C at a heating rate of 10°C min^{-1} under nitrogen atmosphere (flow rate, 20 mL/min). The surface and cross-section images of the films were taken SEM (Hitachi S-4200, Japan) to study the morphological changes. Tensile test specimens were prepared by cutting the films to 10-mm wide and 65-mm long strips using a precise cutter. Tensile test was done on an in-house universal testing machine system under room condition, with a pulling speed of 2 mm/min. Load cell sensor (UU-K010, Daecell, Korea) was used to measure the applied load. Linear scale sensor (GB-BA/SR128-015, Sony, Japan) was used to measure moving distance. The moisture content was tested as follows: a piece of the film about 0.1 g was cut from the whole film, kept in a vacuum oven at 60°C for 12 h, weighed (W_0), and then kept in an environmental chamber. The temperature was controlled at 25°C, and the

TABLE I
Moisture Content (wt %) in Cellulose–Chitosan IPNs Based Actuator Under Different Humidity Environment

Cellulose (% w/w)	Chitosan (% w/w)	Room humidity	50% RH	70% RH	90% RH
100	0	6.33	9.27	11.42	13.75
90	10	8.25	10.34	13.15	15.32
80	20	10.12	10.54	13.88	17.65
70	30	10.86	11.15	15.42	20.25
60	40	12.06	13.24	19.24	26.34
50	50	13.24	15.36	25.36	31.24

humidity was controlled at a certain value (such as 50, 70, and 90%) for 6 h, for saturation, and the film was weighed (W_i). The moisture content (wt %) (W_a) is calculated according formula (1):

$$W_a = (W_i - W_0)/W_0 \times 100\%. \quad (1)$$

The moisture content (wt %) of the films is listed in Table I.

Actuator performance

The electromechanical performance was tested in an environmental chamber that can control temperature and humidity. The bending displacement measurement system consists of a high precision laser doppler vibrometer (LDV) (Brüel&Kjær, 8336), an environmental chamber (KMS, CTH3-2S), a current probe (TCP 300, Tektronix), Labview software on a personal computer, and a function generator (33220A, Agilent).[6] An EAPap actuator is supported vertically in air, and a function generator controlled by computer sends out the excitation AC voltage to the actuator, resulting in a bending deformation. The bending displacement of the EAPap sample is measured by the high precision LDV mounted on an optical table, and the LDV signal is converted to the displacement through the Labview software.

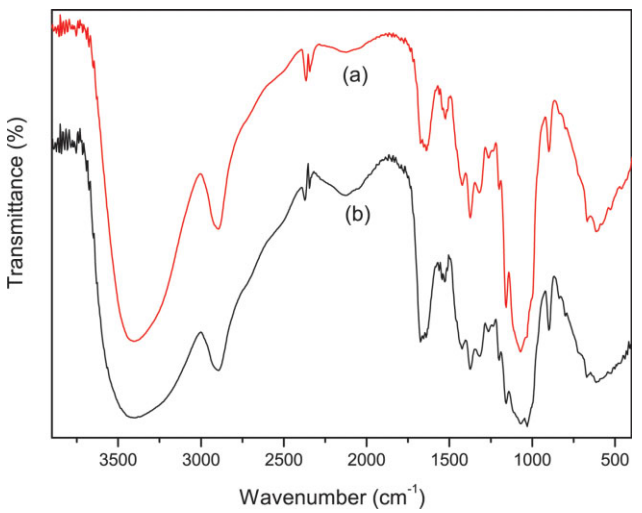

Figure 3 FT-IR spectra of (a) cellulose–chitosan blend and (b) cellulose–chitosan IPN (cellulose–chitsan weight ratio = 50 : 50 wt %). [Color figure can be viewed in the online issue, which is available at www.interscience.wiley.com.]

RESULTS AND DISCUSSION

FT-IR spectra of the cellulose-chitosan blend and cellulose–chitosan IPN were measured to confirm the formation of crosslinking. The cellulose and chitosan weight ratio was 50 : 50 (wt %). Figure 3 depicts the FT-IR spectra of (a) cellulose–chitosan blend and (b) cellulose–chitosan IPN. The cellulose–chitosan blend exhibits a band in the region of 3000–3700 cm^{-1} of the spectrum, corresponding to the stretching of the OH groups. Band at 2820 cm^{-1} represents the aliphatic C—H stretching vibration. Two bands at 1647 and 1375 cm^{-1}, attributed to amide-I and amide-III, characteristic of chitosan with acetylated units are present in all the spectra. Bands at 1575 cm^{-1} represents —NH_2, the free primary amino group of chitosan. A sharp and steep band observed at 1080 cm^{-1} is due to the presence of C—O—C stretching vibrations. All these bands can also be observed in the cellulose–chitosan IPN. A new band observed at 1015 cm^{-1} is due to the presence of an acetal group, which is formed because of the reaction of glutaraldehyde with hydroxyl groups. Thus, FT-IR confirmed the crosslinking reaction of glutaraldehyde with cellulose and chitosan.

Regarding the crystalline structure of cellulose fibers, it is known to be classified into four crystallization types, which can be transformed from one to another. In our previous research,[4] regenerated cellulose films belonged to cellulose II. Cellulose II is well known to be a thermodynamically stable, crystalline cellulose allomorph. Originally, XRD peaks of cellulose II appear at 12.1°, 19.8°, and 22° assigned to (1 1 0), (1 $\bar{1}$ 0), and (2 0 0), and the XRD patterns of cellulose–chitosan blends confirmed that they are cellulose II crystalline.[14]

Figure 4 presents the X-ray diffraction results of cellulose–chitosan IPNs. The patterns are different somewhat from that of cellulose–chitosan blends. The (1 1 0) peak is located at 12.3°, which is higher than that of the cellulose–chitoan blends at 9.8°[14] and DMAc cellulose at 12.1°.[4] With the increasing chitosan content, the peak became weaker and

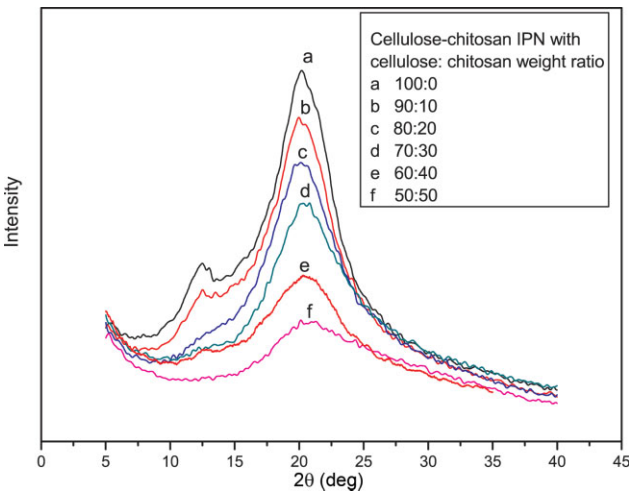

Figure 4 XRD spectra of the cellulose–chitosan IPNs. [Color figure can be viewed in the online issue, which is available at www.interscience.wiley.com.]

finally disappeared after chitosan content was more than 40 wt %. The (1 $\bar{1}$ 0) peak at $2\theta = 19.6°$ can be observed clearly when the chitosan content is lower than 20 wt %. But the (2 0 0) peak at $2\theta = 21.6°$ cannot be detected for all the cellulose–chitosan IPNs. However, a small shoulder peak located around 20.4° appeared when the chitosan content is lower than 30 wt %. This peak should be attributed to the shift of (2 0 0) to lower region. With chitosan content even increasing, (1 $\bar{1}$ 0) peak and (2 0 0) peak were combined to form a new peak at $2\theta = 20.0°$. Compared with (1 $\bar{1}$ 0) peak, this new peak was blunt and the intensity was also decreased. For the IPN case (weight ratio of 50 : 50), the XRD pattern showed an amorphous characteristic. In summary, some structural change might have occured in the cellulose–chitosan IPNs, because of the crosslinked network formation, caused by reaction among cellulose, chitosan, and glutaraldehyde. These network structures can greatly hinder the molecular chains' movement, which in turn decreases the crysallinity of the IPN films. Another considerable reason is the chitosan added in the IPN. On the one hand, chitosan is an amorphous polymer; its effect is like a diluent. On the other hand, the crosslinking could have been occured between the cellulose and chitosan, especially when the chitosan content is high. This crosslinking can also affect the crystallization of cellulose.

To further investigate the crystallinity of the cellulose–chitosan IPN films, we conducted DSC study. DSC thermograms of cellulose–chitosan IPN films with different weight ratio are displayed in Figure 5. In case of pure cellulose IPN, a broad peak is observed at 127°C, which should be due to the recrystallization of cellulose during the heating process.[15] And a small peak located at 320°C is found, which is attributed to the melting transition of the cellulose crystalline. With the introduction of chitosan, the situation has some changes. For 90 : 10 IPN case, the recrystallization temperature is shifted to a higher temperature at 137°C. And at 268°C other crystallization peaks appear. These results indicate that the movement of molecules become harder because of the denser network formation. On the other hand, the melting point is shifted to a lower temperature at 278°C, which means that the crystallinity becomes less regular. With the chitosan content increasing to 20 and 30 wt %, the recrystallization peak becomes more and more small and flat. The melting peak becomes a shoulder peak around 280°C and is followed by decomposition.[16] For the IPN case (weight ratio of 60 : 40), we cannot find any melting peak before decomposition because of the high density of the network.

To investigate the mechanical properties of cellulose–chitosan IPN films, the tensile test was performed. For each IPN ratio, four samples were tested to calculate the average value and derivations. The resultant stress–strain curves of cellulose–chitosan IPN films are presented in Figure 6. When the chitosan content in the IPNs is low (below 30 wt %), we can find the elastic zone and the plastic zone in the stress–strain curves. We can find the yielding point. The elongation at break keeps decreasing

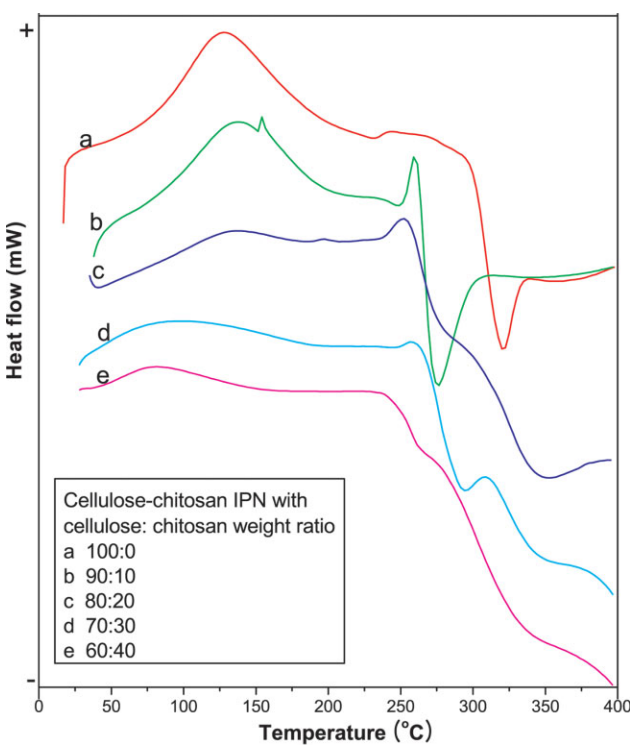

Figure 5 DSC spectra of the cellulose–chitosan IPNs. [Color figure can be viewed in the online issue, which is available at www.interscience.wiley.com.]

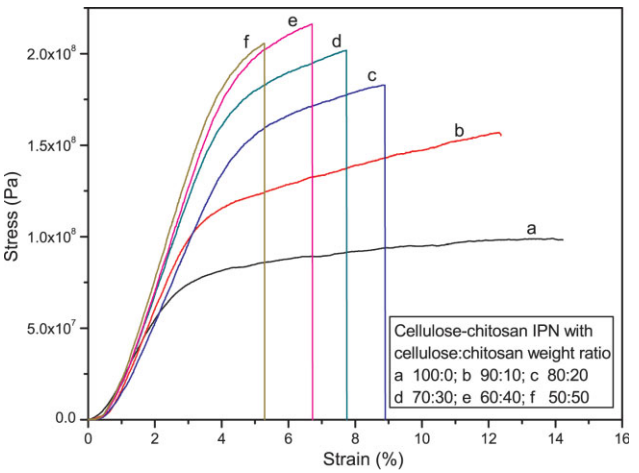

Figure 6 Stress–strain curves of the cellulose–chitosan IPNs. [Color figure can be viewed in the online issue, which is available at www.interscience.wiley.com.]

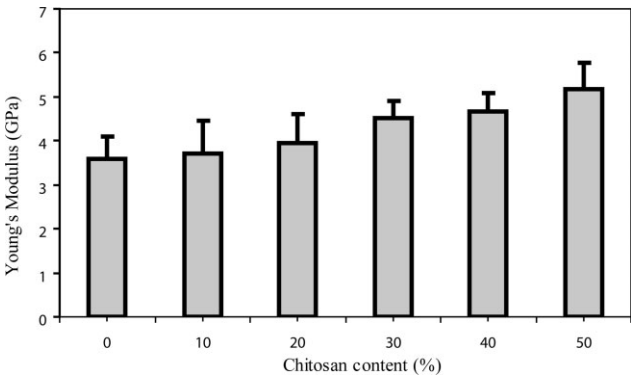

Figure 7 Young's modulus of the cellulose–chitosan IPNs.

from 14.5 to 7.8%, with the chitosan content increasing from 0 to 30 wt %. With the chitosan content even increasing, the plastic zone gradually disappears and only the elastic zone remains. We cannot find the yielding point. The sample becomes hard and brittle since the strain keeps decreasing from 14.5 to 5.2%, whereas the stress keeps increasing from 100 to 200 MPa. These results indicate that with the chitosan content increasing in the IPNs, the crosslink density should be increased.

Figure 7 shows the Young's modulus of the cellulose–chitosan IPN films with chitosan content variation. The Young's modulus was calculated from the slope of elastic zone of the stress–strain curves according to the ASTM D-882-97, as a standard test method for tensile elastic properties of thin plastic sheeting. The value for pure cellulose IPN was about 3.5 GPa. With the increasing chitosan content, the Young's modulus tended to increase slowly, especially for high chitosan content IPN films. These Young's modulus values can be used to calculate the stiffness and resonance frequency of EAPap actuator, which will be discussed later. Moreover, Young's modulus of the crosslinked cellulose and chitosan IPN films can be used to estimate the average molecular weight between crosslinks (M_c), as well as the effective crosslink density (V_e). The M_c was determined using eq. (2).[17]

$$M_c = \frac{3\rho RT}{E}, \tag{2}$$

where ρ is specific density (g/cm^3), R is gas constant, T is absolute temperature, and E is Young's modulus. The effective crosslink density was calculated using the following eq. (3):

$$V_e = \frac{\rho}{M_c}. \tag{3}$$

The results of M_c and V_e estimated for cellulose–chitosan IPN were shown in Table II.

It was noticed that with the increasing chitosan content, the M_c decreased, meanwhile the V_e increased. These results indicated that the network structure became denser. In conclusion, chitosan content significantly affected the crosslink density of IPNs. By changing the chitosan content, we can control the Young's modulus of the IPNs. According to the Ref. 18, the resonance frequency of the EAPap actuator is related to the root of the Young's modulus. Consequently, we can control the resonance frequency of the cellulose–chitosan EAPap actuator in some content.

TABLE II
Results of Tensile-Test of Various Cellulose–Chitosan IPNs

Cellulose (% w/w)	Chitosan (% w/w)	ρ (g/cm^3)	E (GPa)	$M_c \times 10^{-3}$ (kg/mol)	$V_e \times 10^{-2}$ (mol/cm^3)
100	0	0.690	3.58 ± 0.33	16.63 ± 1.62	4.15 ± 0.47
90	10	0.715	3.72 ± 0.51	14.57 ± 1.24	4.91 ± 0.44
80	20	0.734	3.96 ± 0.42	14.05 ± 1.31	5.22 ± 0.36
70	30	0.756	4.51 ± 0.23	12.76 ± 0.72	5.92 ± 0.31
60	40	0.775	4.67 ± 0.27	12.58 ± 0.63	6.16 ± 0.33
50	50	0.800	5.18 ± 0.32	11.71 ± 0.73	6.83 ± 0.35

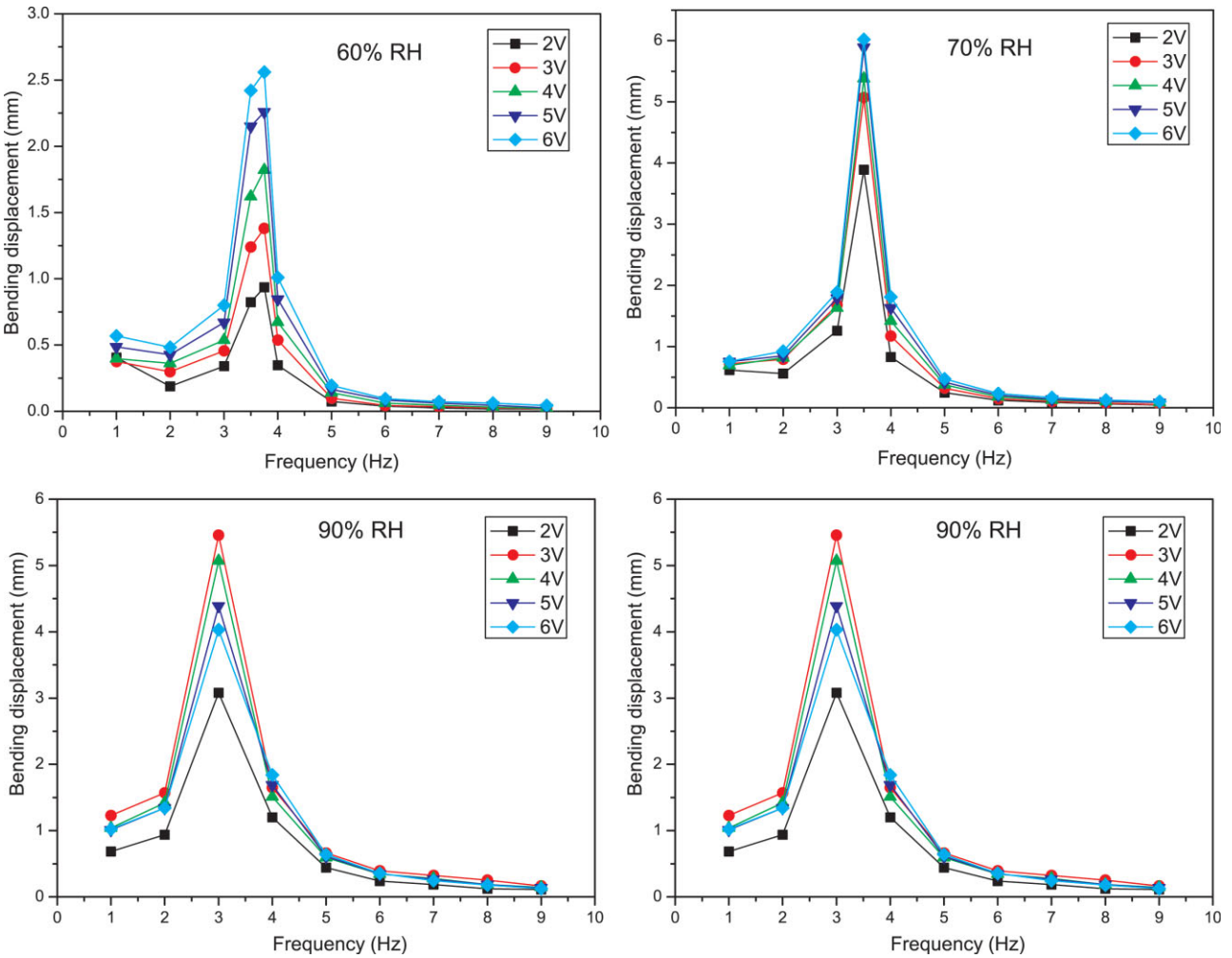

Figure 8 Bending displacement of the cellulose–chitosan IPN actuator with variations in the actuating voltage and frequencies at different relative humidity levels (cellulose–chitosan weight ratio = 60 : 40 wt %). [Color figure can be viewed in the online issue, which is available at www.interscience.wiley.com.]

The bending displacements of the cellulose–chitosan IPN based actuators were measured at the tip of the samples using the laser vibrometer. The test was performed as a function of frequency under different actuating voltage and RH levels. Figure 8 shows the typical actuation behavior of the cellulose–chitosan IPN based actuators with a cellulose and chitosan weight ratio of 60 : 40 under humidity level variations, which ranged from 60 to 90%. The temperature was 25°C and the actuating voltage (peak to peak) ranged from 2 to 7 V. As seen in Figure 6, when the actuating voltage increased, the bending displacement increased. Maximum bending displacement values of 2.7, 6.0, and 7.1 mm were achieved, at maximum actuating voltage, at 60, 70, and 80% humidity conditions, respectively. This was due to the fact that as the actuating voltage increased, the anions moved to the positive electrode quickly, resulting in the increased repulsive force between the anions on the positive electrode, and consequently, increasing the bending displacement. But at 90% RH, the maximum bending displacement of 5.5 mm was achieved at 3 V. Beyond this voltage, the bending displacement rather decreased. The reason was due to the electrode damage at high humidity condition, which will be discussed later. Notice that, the bending displacements showed maximum values at resonance frequencies. As seen in the figure, the resonance frequency changed from 3.8 to 3 Hz with the humidity level increased from 60 to 90%. Resonance frequency of EAPap actuator can be theoretically calculated based on the classical beam theory.[19] The resonance frequency of the EAPap actuator is proportional to the root of the Young's modulus.[18] Usually, the Young's modulus of the film decreases when the humidity content in the film is increased. According to the literature,[20] the Young's modulus is reduced to nearly half when the RH is 99%. Thus, the main reason for decreased resonance frequencies is due to the Young's modulus decrease with the humidity level increase.

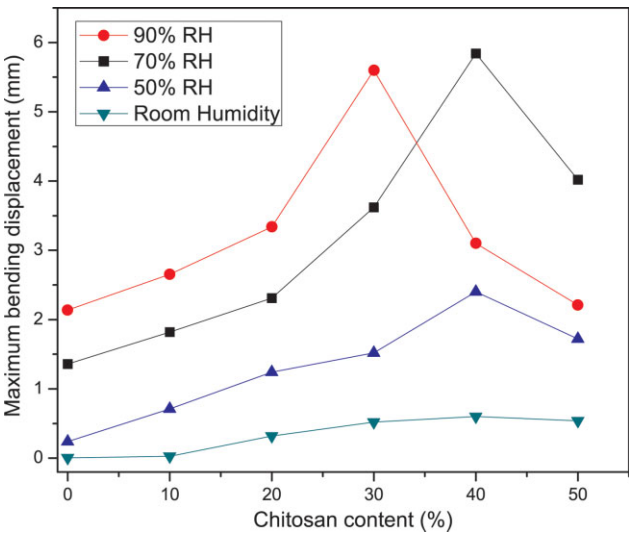

Figure 9 Effect of the chitosan content on the maximum bending displacement of IPNs. (70% RH, 5 V). [Color figure can be viewed in the online issue, which is available at www.interscience.wiley.com.]

Figure 9 shows the maximum bending displacement of IPN based EAPap actuators with the chitsoan content variations under different humidity condition ranging from room humidity to 90% RH. Temperature and actuating voltage of the actuator performance test were fixed at 25°C and 5 V, respectively. With different humidity conditions, the behavior has a little difference. At high humidity condition, the maximum bending displacement increased with the increasing chitosan content, but decreased after 30 wt % in IPN. The optimal chitosan content apparently was around 30 wt %. But at lower humidity condition such as 70 wt % or less, the optimal chitosan content seems to shift to a higher chitosan content region at about 40 wt %.

To explain this behavior, we need to discuss the actuation principle. The actuation principle of EAPap actuators is mainly divided into two parts: the ion migration effect and the piezoelectricity effect. When an external electric field is applied, ions in the amorphous region of the cellulose actuator can be mobile and migrate to the cathode, along with free water molecules in cellulose. Selective ionic and water transport across the cellulose under an electric field results in volumetric changes, which in turn lead to bending. On the other hand, the crystal structure of cellulose II is monoclinic and exhibits piezoelectric properties. It also attributes to the bending actuation.

For cellulose–chitosan IPNs based actuator, as seen from the XRD results, the disordered domains in cellulose–chitosan IPNs increase with the chitosan content increasing, which can improve the ion migration effect. We also check the effect of IPNs hydrophilicity on the bending displacement. Table I shows the water content in the cellulose–chitosan IPNs actuator under different humidity conditions. Apparently, with the chitosan content increasing in the IPNs, the water content in the actuator also increases, which in turn can improve the ion mobility. This is the reason for why the bending displacement of IPNs based EAPap actuator increases with the increased chitosan content. However, when the chitosan content is over about 30–40 wt %, the Young's modulus increase associated with dense network structure surpasses the improvement of the ion migration effect, associated with disordered domains, and the bending displacement decreases. Since the Young's modulus of cellulose–chitosan IPNs is affected by the humidity level, the optimal chitosan content is shifted to a lower region at a high humidity level, such as 90%. Another reason is that at high humidity level, the electrode can be easily damaged leading to deteriorate the bending performance as discussed later.

The durability is an important factor of actuator performance. Another drawback of the cellulose EAPap actuator was the rapid degradation of the performance, which might be associated with solvent residues, electrolytic gas, or electrode damage. Figure 10 represents the bending displacement change of the IPN based EAPap actuator (cellulose–chitosan weight ratio 70 : 30 wt %) with the time variation. Two different humidity levels, 70 and 90% RH, were tested. The temperature was 25°C and actuating voltage was 5 V. The film thickness was 10 ± 2 μm. Before the durability test of the actuator, bending displacements were firstly tested with frequency variations at 5 V to find out the resonance frequencies. When the humidity level was 70% RH,

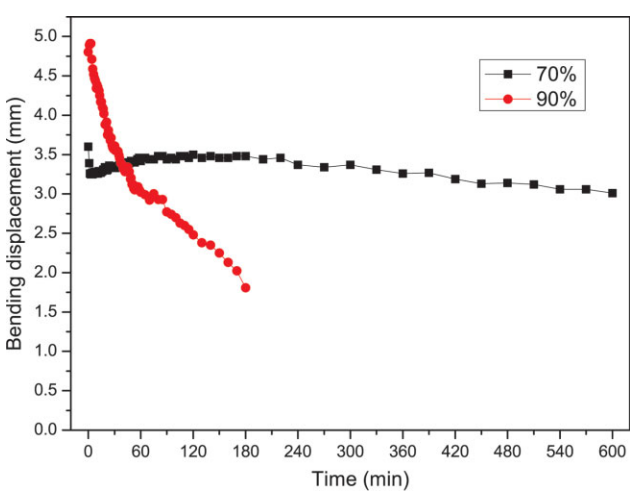

Figure 10 Durability test of the cellulose–chitosan IPN based actuator at different humidity levels (cellulose–chitosan weight ratio = 70 : 30 wt %, 5V). [Color figure can be viewed in the online issue, which is available at www.interscience.wiley.com.]

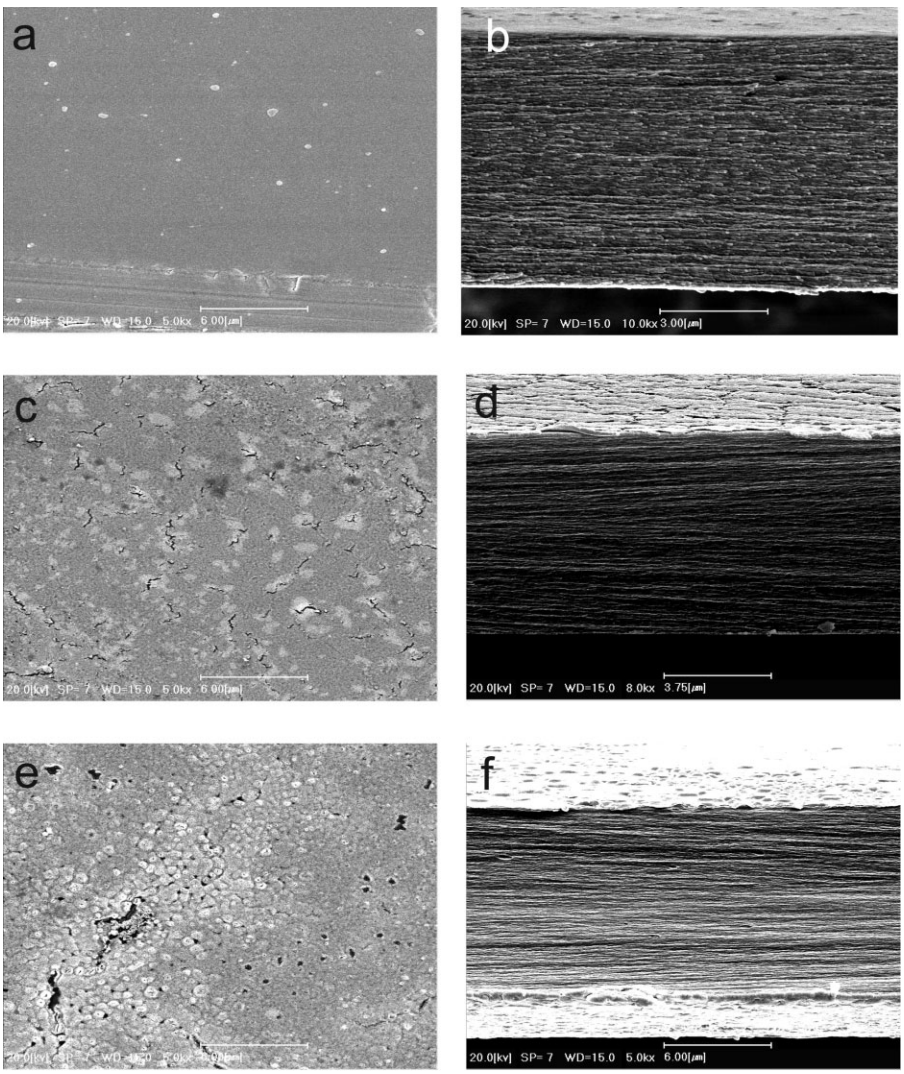

Figure 11 SEM images of the cellulose–chitosan IPN based actuator before and after durability test at different humidity levels [cellulose–chitosan weight ratio = 70 : 30 wt %, 5V; (a, b): surface and cross-section morphology before durability test; (c, d): after durability test at 70% humidity level; and (e, f): after durability test at 90% humidity level].

the resonance frequency was 6 Hz. When the humidity level was increased to 90% RH, the resonance frequency decreased to 4.5 Hz. The durability test was performed at the resonance frequencies. In the 70% RH case, the bending displacement was not large as initially compared with the 90% RH case. It was about 3.6 mm and dropped very quickly to 3.3 mm in few minutes. Then, the bending displacement was increased slowly and saturated to 3.5 mm after about 1 h and kept stable for almost 2 h. Then, it slightly decreased during the next 7 h. The initial drop of the bending displacement may be associated with the initial aging of the material for electrical actuation. After actuation for 10 h, the bending displacement reduction was about 17%. This result is much better than that of the previous result using cellulose–chitosan laminated films as EAPap actuators.[13] In the 90% RH case, the result was different. The initial bending displacement was large, 4.9 mm, compared with the 70% RH case. However, it decreased with time, and the bending displacement reduction was about 60% after 3 h. This result might be associated with gold electrode damage at high humidity level, which will be explained below.

To further investigate the durability, morphology changes of electrodes on the actuator were observed using SEM before and after the durability test at 70 and 90% humidity levels. Figure 11 represents the SEM images at the surface and cross-section of the actuator. Before actuation, the surface morphology of the electrode was rather smooth and compact except for some small holes created by air, dissolved in solvent. Its cross-section morphology was a layer-by-layer structure, which is a typical structure of the regenerated cellulose. And the gold layer was tightly and uniformly attached on the substrate. After

durability test at 70% humidity level for 10 h, numerous small cracks appeared on the whole electrode surface area. For the 90% humidity condition, the situation was even worse. Besides cracks and small holes, numerous small bubbles were formed on the whole electrode surface area. This might be due to the movement of gases or moisture in the sample. The probable source of this bubble formation may be electrolytic gas formation at the metal-polymer interface. From the cross section image, we can see that the adhesion between the electrode layer and substrate was delaminated in some areas. In conclusion, this electrode damage deteriorated the bending displacement and durability. Such a durability problem at high humidity level still remains a challenge in cellulose-based EAPap actuator.

CONCLUSION

Cellulose–chitosan IPN based EAPap actuator was fabricated and its characteristics and the actuator performance were tested. These IPNs were prepared by dissolving cellulose and chitosan with different weight ratios in trifluoroacetic acid as a co-solvent followed by glutaraldehyde treatment. The characteristics of these films were examined by FT-IR, XRD, DSC, and tensile test, which confirmed the formation of IPN. As the chitosan content increased, the crystallinity decreased, the network became denser, and the Young's modulus increased. Bending displacement of the actuators increased with the actuating voltage and humidity level, and maximum bending displacement was achieved at the resonance frequency of the actuator. For a weight ratio of 60 : 40 wt %, a maximum bending displacement of 7.2 mm was found at 80% RH level. Chitosan content in the IPNs significantly affected actuator performance, and the optimum IPN weight ratio of cellulose and chitosan was found to be 60 : 40 wt %. In terms of the durability, the bending lifetime was about 10 h with 17% performance degradation at 70% humidity level. However, the degradation was severe at 90% humidity condition. This was because of the electrode damage at high humidity level. Durability at high humidity condition still remains a challenge for the cellulose based EAPap actuator.

References

1. Klemm, D.; Heublein, B.; Fink, H.-P.; Bohn, A. Angew Chem Int Ed 2005, 44, 3358.
2. Bazhenow, V. A. Piezoelectric Properties of Woods; Consultants Bureau Enterprise Inc.: New York, 1961; p 130.
3. Fukada, E. IEEE Trans Ultrason Ferroelect Freq Control 2000, 47, 1277.
4. Kim, J.; Yun, S.-R.; Ounaies, Z. Macromolecules 2006, 39, 4202.
5. Kim, J.; Seo, Y. B. Smart Mater Struct 2002, 11, 355.
6. Kim, J.; Song, C.; Yun, S.-R. Smart Mater Struct 2006, 15, 719.
7. Kim, J.; Deshpande, S. D.; Yun, S.-R.; Li, Q. Polym J 2006, 38, 659.
8. Deshpande, S. D.; Kim, J.; Yun, S.-R. Synth Met 2005, 149, 53.
9. Yun, S.-R.; Zhao, L. J.; Wang, N. G.; Kim, J. Key Eng Mater 2006, 324, 843.
10. Yun, S.-R.; Kim, J. J Phys D: Appl Phys 2006, 39, 2580.
11. Yun, S.-R.; Kim, J. Smart Mater Struct 2007, 16, 1471.
12. Krajewska, B. J Chem Technol Biotechnol 2001, 76, 636.
13. Kim, J.; Wang, N. G.; Chen, Y. Cellulose 2007, 14, 439.
14. Cai, Z. J.; Kim, J. Smart Mater Struct 2008, 17, 035028.
15. Minoru, K.; Tatsuko, H.; Junzo, N. J Appl Polym Sci 1974, 12, 3069.
16. Groè Be, A. In Polymer Handbook, 3d ed.; Branrup, J.; Immergut, E. H., Eds. Wiley: New York, 1989, p 210.
17. Ward, I. H.; Hadley, D. W. An Introduction to the Mechanical Properties of Solid Polymers; Wiley: Chichester, 1994.
18. Tahhan, M.; Truong, V. T.; Spinks, G. M.; Wallace, G. G. Smart Mater Struct 2003, 12, 626.
19. Rao, S. S. Mechanical Vibrations, 2nd ed.; Addison-Welsy: Reading, MA, 1990; p 398.
20. Mark, R. E. Handbook of Physics and Mechanical Testing of Paper and Paperboard; Dekker: New York, 1989.